

# Thermal Conductivity Evolution of Saturated Clay under Consolidation Process

H. M. Abuel-Naga<sup>1</sup>; D. T. Bergado<sup>2</sup>; and A. Bouazza<sup>3</sup>

**Abstract:** This paper presents the results of a study on the thermal conductivity of a soft saturated clay (Bangkok clay) carried out in relation to an investigation into thermal ground improvement using prefabricated vertical drains. The thermal conductivity of clay specimens was measured, at different porosities and temperature levels, using a simple nondestructive steady-state test method. In addition, a theoretical mixture model to simulate the evolution of thermal conductivity of saturated fine-grained soils has been introduced. It is formulated in terms of thermal conductivity and volume fraction of each soil phase (solid and water), and a morphological parameter controlled by the soil fabric condition. The proposed model has been validated against thermal conductivity results reported in the literature and results obtained from the present investigation. Reasonable agreement has been obtained between the predicted and measured thermal conductivity values.

**DOI:** 10.1061/(ASCE)1532-3641(2008)8:2(114)

**CE Database subject headings:** Thermal resistance; Thermal properties; Heat flow; Clays; Temperature; Soft soils; Soil consolidation; Soil porosity.

## Introduction

A clear understanding of heat transfer through geomaterials is of great interest in many geoengineering projects involving thermal effects, such as oil and gas pipelines (Slegel and Davis 1977), buried high voltage electrical cables (Abdel-Hadi and Mitchell 1981), ground heat energy storage (Moritz 1995), heat exchanger piles (Laloui et al. 2003), and clay barriers for nuclear waste repositories (Gera et al. 1996). The validity and efficiency of an innovative thermal technique capable of enhancing the performance of prefabricated vertical drains in soft Bangkok clay has been investigated recently (Abuel-Naga et al. 2006). For this purpose, a clear understanding of the factors affecting the thermal conductivity of saturated clay and its evolution under the consolidation process is required.

Field or laboratory tests can be used to measure the thermal conductivity of soils (Valente et al. 2006; Côté and Konrad, 2005b; Roth et al. 2004; Newson and Brunning 2004; Naidu and Singh 2004; Abu-Hamdeh et al. 2001; Morin and Silva 1984). However, field tests are expensive, time consuming, and have no

freedom to control the boundary conditions. On the other hand, laboratory tests are relatively inexpensive and simple to conduct. However, great care should be given to soil disturbance and the fitting of the governing equation to the boundary conditions of the test apparatus.

Several researchers (Usovich et al. 2006; Côté and Konrad 2005b; Ochsner et al. 2001; Abu-Hamdeh and Reeder 2000; Brandon and Mitchell 1989; Morin and Silva 1984; Farouki 1981; Sepaskhah and Boersma 1979) have shown that thermal conductivity is related to soil properties such as mineralogical composition, dry density (porosity), pore fluid, degree of saturation, water content, and temperature. The effect of the geometrical arrangement of the soil particles on the thermal conductivity value of the saturated clays has also been discussed by Penner (1963), Mitchell (1993), and Midttømme et al. (1998).

Numerous theoretical and empirical approaches have been developed to model the evolution of the thermal conductivity of two-phase composite material as a function of the thermal conductivity and the volumetric proportions of the different phases as well as their texture (fabric) within the medium. These approaches can also be used to model the evolution of the thermal conductivity of saturated soils. The use of theoretical based models is recommended as the validity of empirical equations is always limited to specific conditions. Appendixes I and II include some of the theoretical mixture models that have been developed to simulate the thermal conductivity of the two-phase system. The models listed in Appendix I were derived without taking into consideration the fabric configuration effects on the thermal conductivity. Fig. 1 shows the feature of these models in the thermal conductivity-porosity ( $\lambda_T-n$ ) plane. The parallel and series heat flow modes can be considered as the upper and lower bound of the theoretical models as shown in Fig. 1.

On the other hand, the models listed in Appendix II are flexible in terms of considering different fabric conditions since they include fabric parameters. However, they also have some limitations. According to Johansen (1975), the values of the shape factors used by De Vries (1963) were empirical since they can hardly

<sup>1</sup>Senior Lecturer, Dept. of Civil and Environmental Engineering, Faculty of Engineering, The Univ. of Auckland, Private Bag 92019, Auckland Mail Centre, Auckland 1142, New Zealand (corresponding author). Email: hossam.abuelnaga@gmail.com

<sup>2</sup>Professor, School of Engineering and Technology, Asian Institute of Technology, P.O. Box 4, Khlong Luang, Pathumthani 12120, Thailand. E-mail: bergado@ait.ac.th

<sup>3</sup>Associate Professor, Dept. of Civil Engineering, Building 60, Monash Univ., Melbourne, Vic. 3800, Australia. E-mail: malek.bouazza@eng.monash.edu.au

Note. Discussion open until September 1, 2008. Separate discussions must be submitted for individual papers. To extend the closing date by one month, a written request must be filed with the ASCE Managing Editor. The manuscript for this paper was submitted for review and possible publication on June 5, 2006; approved on August 7, 2007. This paper is part of the *International Journal of Geomechanics*, Vol. 8, No. 2, April 1, 2008. ©ASCE, ISSN 1532-3641/2008/2-114-122/\$25.00.

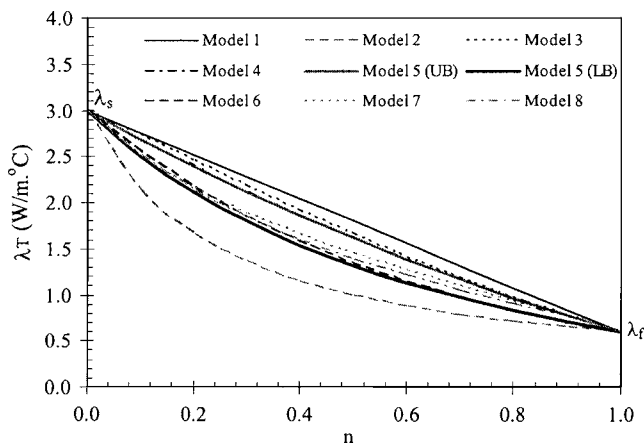


Fig. 1. Feature of different theoretical thermal conductivity mixture models in  $\lambda_T$ - $n$  plane

represent the geometrical shape of sand particles. Kumlutas et al. (2003) show that the Lewis and Nielsen (1970) model underpredicts the thermal conductivity. The model proposed by Hsu et al. (1995) was entangled by linking its fabric parameters to the soil porosity (Ma et al. 2003). Finally, the large number of parameters in Yu and Cheng (2001) model hindered its applicability. Based on the above discussion, it can be concluded that a simple thermal conductivity model that can overcome the limitations of the available models is required.

The objective of this paper is to present a simple nondestructive method to measure the thermal conductivity of saturated soils under steady-state conditions using a modified oedometer cell. In addition, the thermal conductivity evolution of saturated fine-grained soils under a consolidation process is modeled in terms of thermal conductivity and volume fraction of each soil phase, and a morphological parameter that determine the share of both extreme heat flow models (series/parallel) controlled by the soil fabric condition.

## Equipment and Procedure

Mitchell and Kao (1978) reviewed most of the methods used to evaluate the thermal conductivity of soils. These methods can be classified into two main categories, namely: steady-state methods and unsteady-state methods. The steady-state methods measure the thermal conductivity when the temperature of a soil specimen, subjected to a temperature gradient, is constant with time at any point and the heat flux through the soil specimen reaches a constant level. In contrast, the unsteady-state methods measure the thermal conductivity during the transient state. The steady-state method was adopted in this study.

The proposed thermal conductivity cell consists of a modified oedometer that can control different temperature levels on both sides of the soil specimen as shown in Fig. 2. The diameter and the height of the tested specimen are 50.0 and 20.0 mm, respectively. The specimen porosity can be decreased by increasing the vertical pressure. The required temperature gradient through the soil specimen was generated using a constant temperature hot water chamber located on the top of the specimen while the bottom of the specimen was in direct contact with a heat sink at constant lower temperature. A calibrated Captec heat flux transducer (diameter=50.0 mm, sensitivity=10  $\mu\text{V}/\text{W}/\text{m}^2$ ) was placed between the bottom of the soil specimen and the heat sink

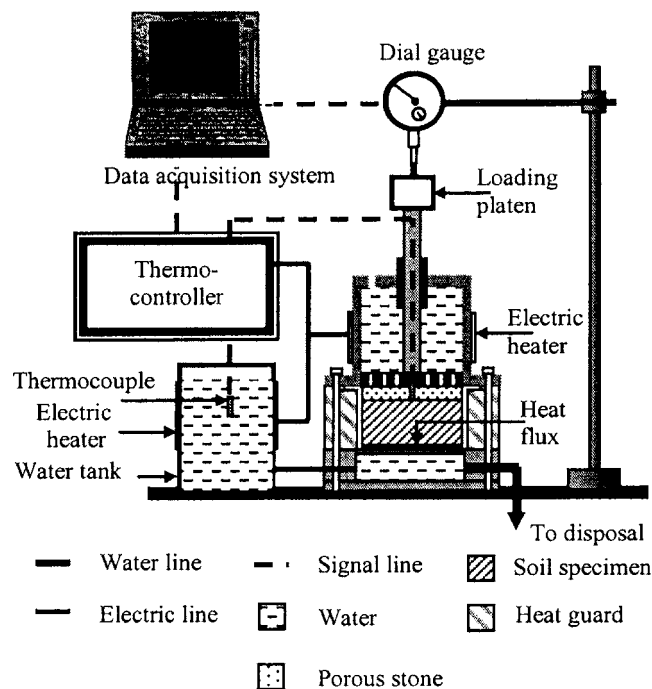


Fig. 2. Schematic of thermal conductivity apparatus

to measure the axial heat flux through the soil specimen under the imposed temperature gradient. To provide one-dimensional heat flow condition through the soil specimen a guard furnace (thermal conductivity=0.018  $\text{W}/\text{m} \cdot ^\circ\text{C}$ , thickness=50.0 mm) was installed around the test specimen to eliminate lateral heat transfer. The proposed test apparatus offers the following advantages:

1. The thermal interface resistance is eliminated by using the temperature controlled water at the upper surface of the soil sample. Moreover, application of a confined stress reduces the interface resistance at the lower surface of the sample; and
2. The effect of water migration under a temperature gradient on the measured thermal conductivity is eliminated due to the presence of temperature controlled water at the upper surface of the soil sample and an undrained surface at the bottom of the soil sample.

The thermal conductivity value under one-dimensional heat flow condition,  $\lambda_T$  ( $\text{W}/\text{m} \cdot ^\circ\text{C}$ ), can be expressed using Fourier's law of heat conduction as follows

$$\lambda_T = \frac{q}{\Delta T/L} \quad (1)$$

where  $q$  ( $\text{W}/\text{m}^2$ )=heat flux through the soil specimen at steady state condition;  $\Delta T$  ( $^\circ\text{C}$ )=imposed temperature difference; and  $L$  (m)=soil specimen thickness. The heat flux at steady-state condition can be determined from the heat flux ( $q$ ) versus time ( $t$ ) plot as shown in Fig. 3. The general shape of the  $q$ - $t$  plot includes two regions, namely: unsteady-state and steady-state zones. The unsteady-state zone refers to the case where the heat flux increases with time, whereas the steady-state zone starts when the heat flux levels off to a constant value.

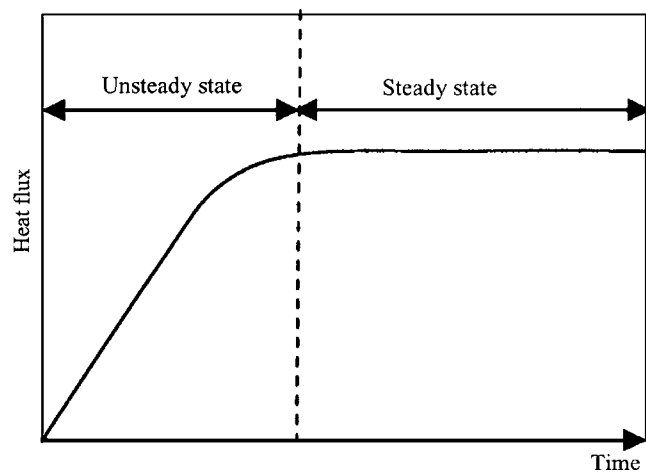


Fig. 3. Typical experimental heat flux behavior

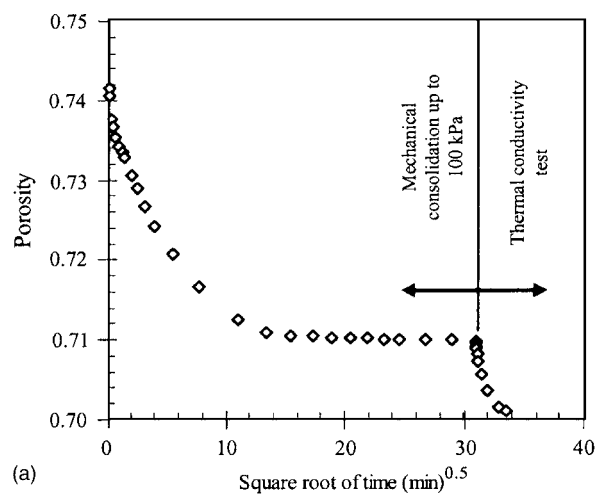
### Soil Specimen and Experimental Program

Undisturbed specimens of soft Bangkok clay used in this study were obtained from 3.0 to 4.0 m depth in the soft clay layer. The physical properties of this soil are presented in Table 1. The mineralogical composition of this clay was investigated by Ohtsubo et al. (2000). The results show that soft Bangkok clay consists of smectites ranging from 54 to 71%, kaolinites (28–36%), and micas.

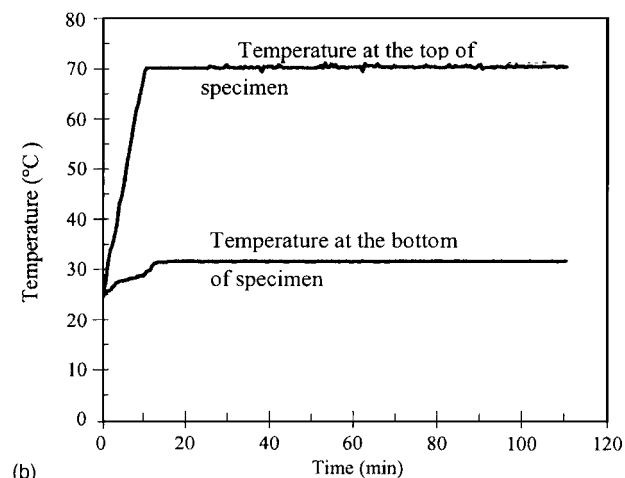
The proposed experimental work was directed to study the effect of porosity and temperature levels on the measured thermal conductivity value under saturated conditions. The experimental program involved measurements of thermal conductivity of three sets of specimens (each set consisted of four specimens), where the direction of mechanical loading and heat flow was parallel to the depositional direction of the soil. Different temperature gradients (30–50, 30–70, and 30–90°C) were applied to the clay specimens, consolidated under different vertical stress levels (100, 200, 300, and 400 kPa, respectively). The thermal conductivity test was started at the end of the primary consolidation stage (for each stress level) by inducing the required temperature gradient. This latter was achieved by setting up a high temperature at the top of the specimen and a low temperature at the bottom of the specimen.

Table 1. Characteristic Value of Soft Bangkok Clay

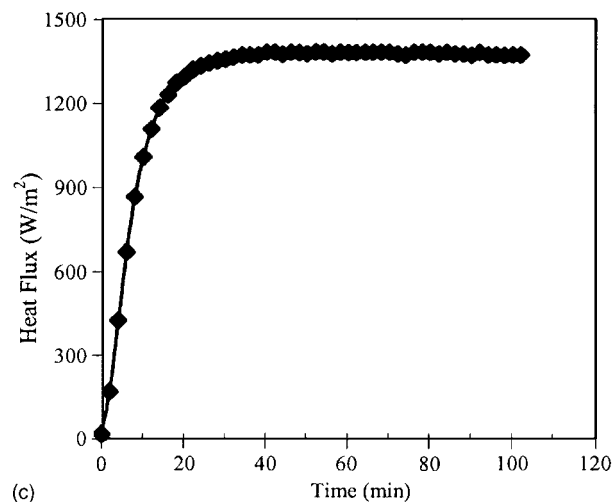
Properties	Value
Liquid limit (LL) (%)	103
Plastic limit (PL) (%)	43
Plasticity index (PI) (%)	60
Natural water content (%)	90
Sensitivity	7.4
Grain size distribution	
Clay (%)	69
Silt (%)	28
Sand (%)	3
Specific gravity	2.68
Color	Dark grey



(a)



(b)



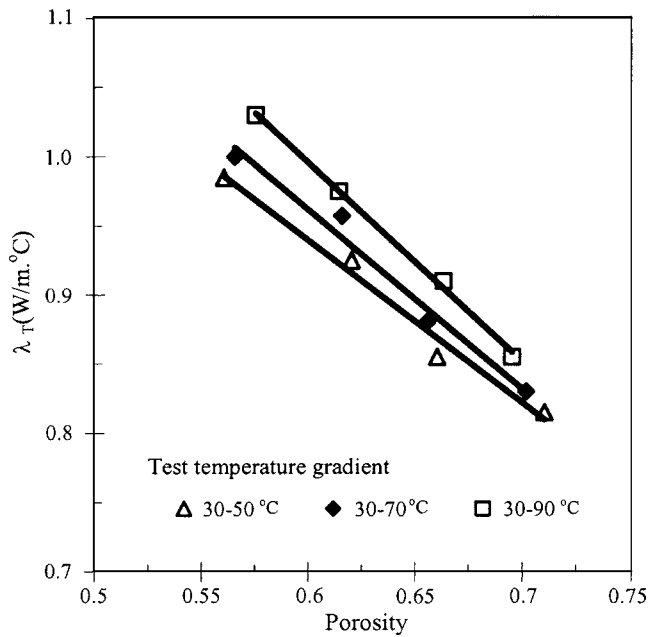
(c)

Fig. 4. Typical test results obtained on clay specimen under 100 kPa vertical stress and 30–70°C temperature gradient

## Results and Discussion

### Effect of Porosity and Temperature on Thermal Conductivity

Fig. 4 shows typical measurements made during thermal conductivity tests. Fig. 4(a) illustrates the variation of porosity versus time due to vertical effective stress and temperature gradient that



**Fig. 5.** Porosity and temperature effect on thermal conductivity of soft Bangkok clay

was imposed during the thermal conductivity test. The imposed temperature gradient and heat flux versus time are shown in Figs. 4(b and c), respectively. Figs. 4(b and c) indicate that the designated temperature gradient and heat flux reached a steady-state condition in approximately 15 and 40 min, respectively. The variation of thermal conductivity ( $\lambda_T$ ) versus soil porosity ( $n$ ), for different temperature gradients, is shown in Fig. 5. The results indicate that for a given temperature gradient, as the porosity decreases the thermal conductivity increases. The observed trend is consistent with previous work reported in the literature (Morin and Silva 1984; Midttømme et al. 1998). The variation of the thermal conductivity with porosity under saturated conditions can be attributed to the difference in the thermal conductivity coefficient of the soil pore fluid and soil particles. The soil pore fluid, which consists of water, has lower thermal conductivity than the soil minerals (Horai 1971; Brigaud and Vasseur 1989; Mitchell 1993). Since decreasing porosity under saturated conditions leads to water content reduction, the overall thermal conductivity of the soil specimen will tend to increase. The same figure also indicates that the thermal conductivity values increase as the average soil temperatures increases. Similar results have been reported by Sepaskhah and Boersma (1979) and Morin and Silva (1984). Morin and Silva (1984) demonstrated experimentally that the thermal evolution of thermal conductivity for different saturated soil types can be mainly attributed to the change in the water thermal conductivity with temperature. Therefore, the thermal conductivity of the soil solid phase can be considered as temperature independent.

### Modeling Evolution of Thermal Conductivity under Consolidation Process

The following assumptions were adopted to develop the proposed thermal conductivity model:

1. The soil is fully saturated. Consequently, it can be expressed as a two-phase system;

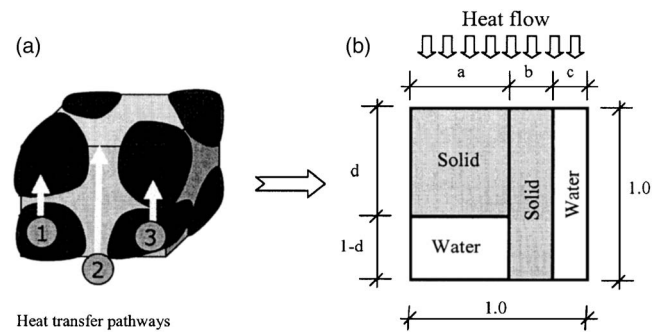


**Fig. 6.** Conceptual model of heat flow through saturated porous media

2. Only heat transfer by conduction is considered since the heat transfer by convection and radiation can be neglected as the clay hydraulic conductivity is very small and the soil is fully saturated, respectively;
3. The parallel and series heat flow models can be considered as the two extreme theoretical model equations of saturated soil thermal conductivity, as shown in Fig. 1 (McGaw 1969; Hadley et al. 1984);
4. The consolidation process only induces changes in soil porosity, whereas the preferred soil particle orientation, size, and shape are not affected (Meade 1966; McConnachie 1974; Martin and Ladd 1975; Anandarajah and Kuganenthira 1995); and
5. Thermal conductivity of the soil minerals are temperature independent while the thermal conductivity of water is temperature dependent.

Under the above assumption, the heat conduction through saturated soils can be expressed through three paths, as shown in Fig. 6(a), namely: (1) a series path through the solid particles that are thought to be bridged by portions of the pore fluid; (2) a continuous path through the portion of the pore fluid; and (3) direct transfer from solid to solid connections between particles. Therefore, under one-dimensional heat flow conditions, the unit cell of saturated porous media [Fig. 6(a)] can be conceptualized, as shown in Fig. 6(b). The thermal conductivity of the proposed conceptual unit cell [Fig. 6(b)] can be expressed under the framework of Ohm's Law as follows

$$\lambda_T = \frac{a}{\frac{d}{\lambda_s} + \frac{1.0-d}{\lambda_f}} + b\lambda_s + c\lambda_f \quad (2)$$

where  $d$  = contribution of the solid phase to the series flow. The terms  $a$ ,  $b$ , and  $c$ , respectively, indicate ratios of the three paths of heat conduction through the saturated soils to the total heat conduction ( $a+b+c=1.0$ ). The volume of solid ( $v_s$ ) and the volume of water ( $v_w$ ) can be expressed as follows

$$v_s = 1 - n = ad + b \quad (3)$$

$$v_w = n = c + a(1 - d) \quad (4)$$

The difficulty in the determination of  $a$ ,  $b$ , and  $d$  from experimental measurements restrict the applicability of Eq. (2). Therefore, some reasonable assumptions are required in order to simplify the general series-parallel model.

Eq. (2) shows that the thermal conductivity of saturated soils is expressed by some combination of the parallel and series heat flows. A simple approach called the weighted series-parallel heat



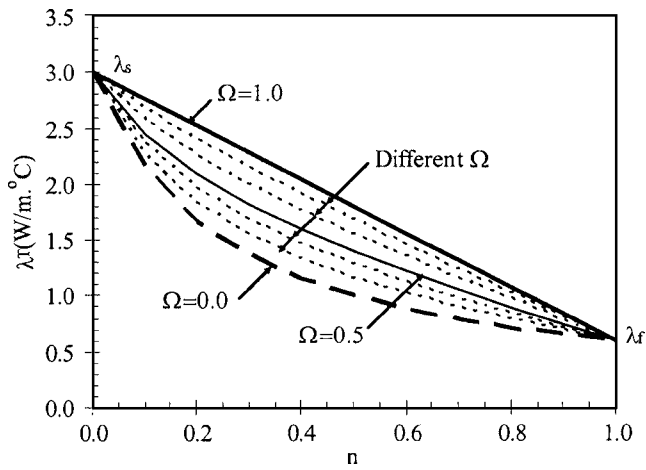


**Fig. 7.** Proposed thermal conductivity model behavior at different morphological soil parameter  $\Omega$

flow model is proposed in this study to predict the thermal conductivity of saturated soils. The proposed approach assumes that the thermal conductivity of soils can be expressed with a weighted combination of the two extreme heat flow conditions (series/parallel) as follows

$$\lambda_T = \Omega \lambda_T^{\text{Parallel}} + (1 - \Omega) \lambda_T^{\text{Series}} \quad (5)$$

where  $\lambda_T^{\text{Parallel}}$  and  $\lambda_T^{\text{Series}}$  = thermal conductivity using the parallel and series model, respectively; and  $\Omega$  = morphological soil parameter that determines the share of both extreme heat flow models (series/parallel) with  $0.0 \leq \Omega \leq 1.0$ . Therefore, the following relationship can be deduced

$$\Omega = \frac{V_s^{\text{parallel}}}{V_s} = \frac{V_f^{\text{parallel}}}{V_f} \quad (6)$$

where the terms  $V_s$ ,  $V_f$ ,  $V_s^{\text{parallel}}$ , and  $V_f^{\text{parallel}}$  = total volume of solid and water, and the volume of solid and water in the parallel heat flow path, respectively. Consequently, the parameters of the general series/parallel model [Eq. (2)] can also be expressed using the weighted approach as follows

$$b = \Omega(1 - n) \quad (7)$$

$$c = \Omega n \quad (8)$$

$$a = 1 - \Omega \quad (9)$$

$$d = 1 - n \quad (10)$$

Therefore, Eq. (6) can be presented in the following form using the proposed weighted approach

$$\lambda_T = \frac{1 - \Omega}{\frac{1 - n}{\lambda_s} + \frac{n}{\lambda_f}} + \Omega[(1 - n)\lambda_s + n\lambda_f] \quad (11)$$

The above equation can be reduced to the parallel and series heat flow model if  $\Omega$  is set to 1.0 and 0.0, respectively. However, the values of  $\Omega$  between 0.0 and 1.0 represent the series-parallel heat flow condition with different combination degrees of the two extreme limits, as shown in Fig. 7. The space between the two extreme limits (series/parallel heat flow) expresses the possible zone of thermal conductivity value for the soil in the  $\lambda_T$ - $n$  plane.

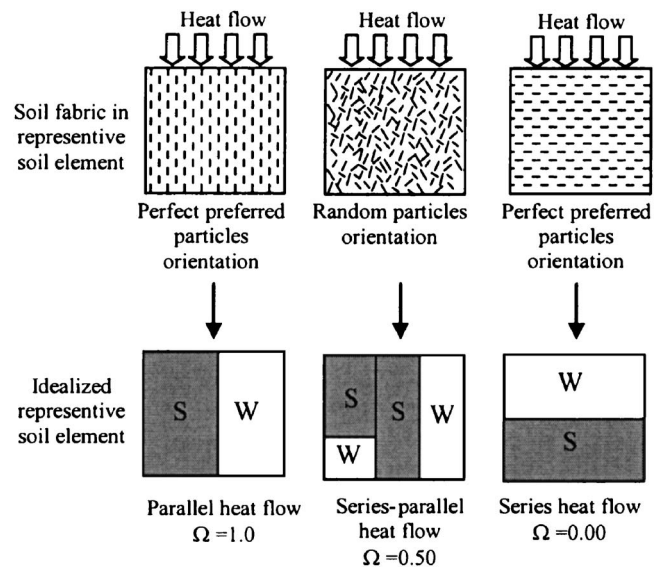


**Fig. 8.** Interpretation of soil fabric using morphological soil parameter  $\Omega$

### Physical Meaning of $\Omega$

Since the proposed parameter  $\Omega$  was used to describe the share of both extreme heat flow models (series/parallel) which could be controlled by the preferred soil particle orientation, the parameter  $\Omega$  can also be used as an indirect indication of soil fabric anisotropy as follows (Fig. 8)

$$\Omega = 0.0$$

The preferred soil particle's orientation is normal to the heat flow direction (anisotropic thermal conductivity condition).

$$\Omega = 0.5$$

Soil particles have random orientation (isotropic thermal conductivity condition).

$$\Omega = 1.0$$

The preferred soil particle's orientation is parallel to the heat flow direction (anisotropic thermal conductivity condition).

### Determination of Model Parameters

Three model parameters are required to predict the thermal conductivity of a saturated soil using the proposed model [Eq. (11)], namely; mean thermal conductivity value of soil solid components ( $\lambda_s$ ), thermal conductivity value of fluid component ( $\lambda_f$ ), and morphological soil parameter  $\Omega$ . In fact, the soil solid phase consists of various soil particles that have different mineral types. The thermal conductivities of common minerals are listed in Table 2 (Horai 1971; Brigaud and Vasseur 1989). Therefore, the mean thermal conductivity of the solid soil phase,  $\lambda_s$ , can be determined using one of the averaging methods. Kasubuchi (1984) investigated three averaging methods and concluded that the weighted geometric mean yields the best approximation for the mean thermal conductivity of the solid soil phase. The weighted geometric mean is expressed as follows

$$\lambda_s = \lambda_{sa}^{v_{sa}} \lambda_{sb}^{v_{sb}} \quad (12)$$

where  $\lambda_{sa}$  and  $\lambda_{sb}$  = thermal conductivity of the constituents  $a$  and  $b$ , respectively. The terms,  $v_{sa}$  and  $v_{sb}$  = volumetric ratio of con-

**Table 2.** Thermal Conductivity of Common Minerals (Data from Horai 1971)

Mineral	Thermal conductivity (W/m °C)
Quartz	7.8
Calcite	3.4
Dolomite	5.1
Anhydrite	6.4
Pyrite	19.2
Siderite	3.0
Orthoclase	2.3
Albite	2.3
Halite	6.5
Mica	2.3
Chlorite	5.1
Kaolinite	2.8
Smectite	1.8
Illite	1.8
Air	0.03
Water	0.60

stituents  $a$  and  $b$  in the soil sample, respectively, and

$$v_{sa} + v_{sb} = 1 \quad (13)$$

The thermal conductivity of water increases with temperature up to 130 °C. Tarnawski et al. (2000) have proposed the following equation to predict the thermal conductivity of water ( $\lambda_f$ ) in W/m °C at different temperature levels where  $T_c$ =water temperature in °C

$$\lambda_f = 0.569 + (1.884 \times 10^{-3})T_c - (0.0772 \times 10^{-5})(T_c)^2 \quad (14)$$

The morphological parameter  $\Omega$  can be determined using the back-calculation approach [Eq. (11)] that required the test results of one thermal conductivity test at known porosity. However, by conducting two thermal conductivity tests at different porosities, Eq. (11) can be also used to determine both  $\lambda_s$  and  $\Omega$ . Taking into consideration the expected variation in the range of the soil mineral composition and the validity of the weighted geometrical mean approach [Eq. (12)], the back-calculation approach for predicting  $\lambda_s$  is highly recommended.

## Validation of Proposed Model

### Soft Bangkok Clay

The model parameters for soft Bangkok clay obtained by back-calculation are:  $\lambda_s = 1.92$  W/m °C and  $\Omega = 0.4$ . The thermal conductivity of water ( $\lambda_f$ ) was estimated to be 0.66 W/m °C using Eq. (14) where the average soil temperature due to the imposed temperature gradient (30–70 °C) is 50 °C. Fig. 9 shows reasonable agreement between the thermal conductivity test results and the model predictions. The resulting value of  $\Omega$  suggest that the soft Bangkok clay has random particles orientation. Lambe (1958) states that sedimentation in a high electrolytic concentration leads to flocculated structure (random soil particle orientation), it is expected that the Bangkok clay will have a flocculated structure as it is of marine deposits origin. Moreover, the study conducted by Collins and McGown (1974) on a variety of natural soils shows that for very sensitive soils the book-house and flocculated structure are observed. Therefore, the higher sensitivity value of soft Bangkok clay ( $S=7.4$ , see Table 1) can be used as an indicator to its flocculated structure.

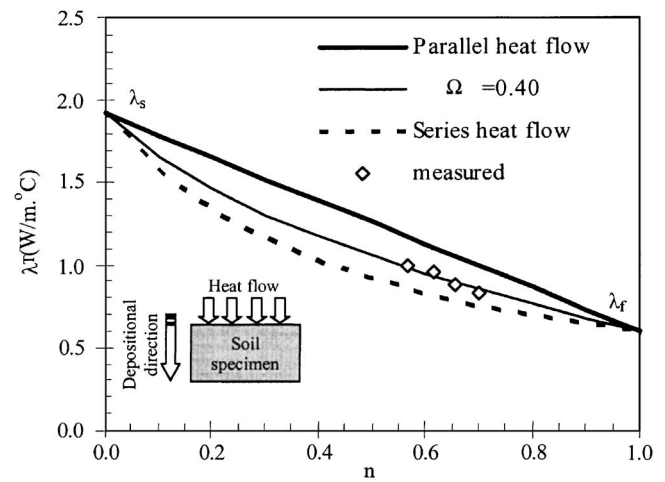


**Fig. 9.** Measured and model prediction thermal conductivity results of undisturbed soft Bangkok clay

culated structure are observed. Therefore, the higher sensitivity value of soft Bangkok clay ( $S=7.4$ , see Table 1) can be used as an indicator to its flocculated structure.

### Illitic Clay

Morin and Silva (1984) measured the thermal conductivity of undisturbed Illitic clay specimens taken from large-diameter gravity cores retrieved from the north-central Pacific. The model parameters for Illitic clay obtained by back-calculation are:  $\lambda_s = 2.5$  W/m °C,  $\Omega = 0.45$ . The thermal conductivity of water ( $\lambda_f$ ) was estimated to be 0.60 W/m °C. The measured thermal conductivity values and the proposed model predictions have been plotted in Fig. 10. A close agreement can be observed between the measured and predicted thermal conductivity values. The  $\Omega$  value indicates that the soil particles tend to have random orientation. Since the Illitic clay is a marine deposit, the preferred soil particles orientation deduced from the proposed model is consistent with present opinion about the influence of sedimentation environment on clay particle arrangement in clay deposits.

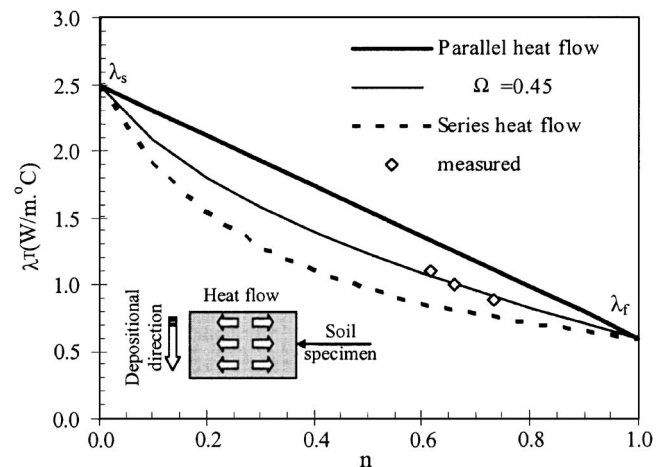


**Fig. 10.** Measured and model prediction thermal conductivity results of undisturbed Illitic clay (data from Morin and Silva 1984)

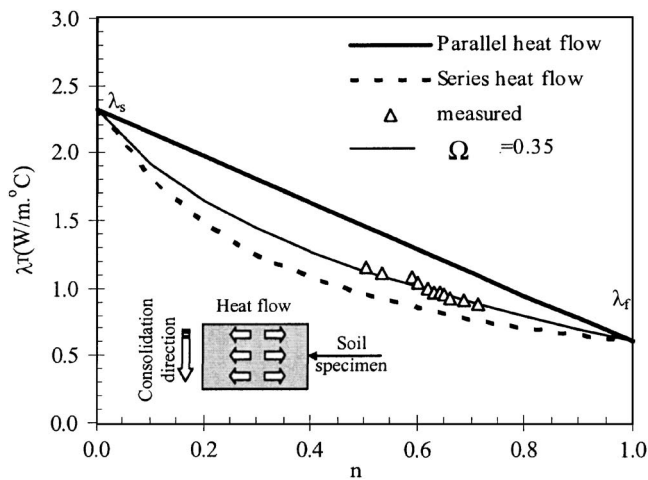


**Fig. 11.** Measured and model prediction thermal conductivity results of highly disturbed (fluidized) North Sea clay (data from Newson and Brunning 2004)

### North Sea Clay Sediment

Newson and Brunning (2004) measured the thermal conductivity of highly disturbed (fluidized) deep water offshore North Sea clay sediments. The soil used for these tests was grey silty clay with liquid limit of 57%, plastic limit of 28%, and specific gravity of the soil of 2.66. Fig. 11 compares the test results and the proposed model predictions where the model parameters  $\lambda_s$  and  $\Omega$  obtained by back-calculation approach are 2.32 W/m °C and 0.35, respectively, and using  $\lambda_f=0.60$  W/m °C. Reasonable agreements can be observed between the test results and the model predictions.

### Conclusions

This study presents a simple nondestructive steady-state method to measure the thermal conductivity of saturated clays. The effects of porosity and temperature levels on the thermal conductivity of soft Bangkok clay have been investigated using a modified oedometer. The salient conclusions that can be drawn from this investigation are as follows:

1. The thermal conductivity increased as the soil porosity decreased. This is due to the difference in the thermal conductivity coefficient of the soil pore fluid and soil solid phase; and
2. The thermal conductivity also increased as the soil temperature increased due to the increase in thermal conductivity of water with temperature.

More importantly, a simple model has been introduced in this study to simulate the evolution of thermal conductivity of saturated clays under the consolidation process. It is expressed in terms of the thermal conductivity and volume fractions of each soil phase and a morphological parameter that determine the mixing ratio of both extreme heat flow models (series/parallel) which are controlled by the soil fabric condition. The proposed model has been validated using the thermal conductivity test results obtained with soft Bangkok clay and test results reported in the literature. The predictions of the proposed model reasonably agreed with the measured results.

### Appendix I

The theoretical thermal conductivity mixture models (two-phase system) that do not include soil particles fabric effect are as follows, where  $\lambda_T$ ,  $\lambda_s$ , and  $\lambda_f$ =thermal conductivity of the soil, solid soil particles, and soil pore water, respectively. The term  $n$  and  $\phi$ =soil porosity and volumetric fraction of solid particles ( $\phi=1-n$ ), respectively.

Model No. 1: Parallel heat flow

$$\lambda_T = n\lambda_f + (1-n)\lambda_s$$

Model No. 2: Series heat flow (Reuss 1929)

$$(\lambda_T)^{-1} = n\lambda_f^{-1} + (1-n)\lambda_s^{-1}$$

Model No. 3: Russell (1935)

$$\lambda_T = \lambda_s \left[ \frac{n^{2/3} + (\lambda_s/\lambda_f)(1-n^{2/3})}{n^{2/3} - n + (\lambda_s/\lambda_f)(1+n-n^{2/3})} \right]$$

Model No. 4: Maxwell (1954)

$$\lambda_T = \lambda_s \left[ \frac{\lambda_f + 2\lambda_s + 2n(\lambda_f - \lambda_s)}{\lambda_f + 2\lambda_s - n(\lambda_f - \lambda_s)} \right]$$

Model No. 5: Hashin and Shtrikman (1962)

$$\lambda_{TU} = \lambda_s + \frac{n}{\frac{1}{\lambda_f - \lambda_s} + \frac{1-n}{3\lambda_s}} \quad \lambda_{TL} = \lambda_f + \frac{1-n}{\frac{1}{\lambda_s - \lambda_f} + \frac{n}{3\lambda_f}}$$

where  $\lambda_{TL}$  and  $\lambda_{TU}$ =lower and upper bound, respectively.

Model No. 6: Geometric mean method (McGaw 1969; Côté and Konrad 2005a)

$$\lambda_T = \lambda_s^{(1-n)}(\lambda_f)^n$$

Model No. 7: Nimick and Leith (1992)

$$\lambda_T = \lambda_{TL} \left[ 1 - \frac{3n(1-A)}{2+A+n(1-A)} \right] \quad A = \frac{\lambda_{TU}}{\lambda_{TL}}$$

$\lambda_{TL}$  and  $\lambda_{TU}$  are from the model of Hashin and Shtrikman (1962).

Model No. 8: Tarnawski et al. (2000) and Gori and Corasaniti (2004)

$$\frac{1}{\lambda_T} = \frac{\beta-1}{\lambda_f\beta} + \frac{\beta}{\lambda_f[\beta^2-1] + \lambda_s} \quad \beta = \sqrt[3]{\frac{1}{1-n}}$$

### Appendix II

The theoretical thermal conductivity mixture models (two-phase system) that include soil particles fabric effect are as follows:

Model No. 9: De Vries (1963)

$$\lambda_T = \frac{n\lambda_f + \sum_{i=1}^N k_i\phi_i(\lambda_s)_i}{n + \sum_{i=1}^N k_i\phi_i}$$

where  $N$ =number of individual types of soil solid components; and  $K$ =soil particle shape factor.

Model No. 10: Lewis and Nielsen (1970) and Kumlutas et al. (2003)

$$\lambda_T = \lambda_f \frac{1 + a \cdot b \cdot \phi}{1 - b \cdot \phi \cdot \psi} \quad b = \frac{(\lambda_s/\lambda_f) - 1}{(\lambda_s/\lambda_f) + a} \quad \psi = 1 + \left( \frac{1 - \phi_m}{\phi_m^2} \right) \cdot \phi$$

where  $a$  and  $\phi_m$  = fabric parameters and maximum volumetric fraction of solid particles, respectively.

Model No. 11: Hsu et al. (1995)

$$\lambda_T = \lambda_f \left[ 1 - \gamma_a^2 - 2\gamma_a\gamma_c + 2\gamma_a^2\gamma_c + \frac{\gamma_c^2\gamma_a^2}{1/\left(\frac{\lambda_s}{\lambda_f}\right)} + \frac{\gamma_a^2 - \gamma_a^2\gamma_c^2}{1 - \gamma_a + \gamma_a/\left(\frac{\lambda_s}{\lambda_f}\right)} + \frac{2(\gamma_a\gamma_c - \gamma_a^2\gamma_c)}{1 - \gamma_a\gamma_c + \left(\gamma_a\gamma_c/\left(\frac{\lambda_s}{\lambda_f}\right)\right)} \right]$$

where  $n = (1 - 3\gamma_c^2)\gamma_a^3 + 3\gamma_c^2\gamma_a^2$ , and  $\gamma_a$  and  $\gamma_c$  = fabric parameters related to the particle geometry and the particle contact, respectively.

Model No. 12: Yu and Cheng (2001)

$$\lambda_T = \lambda_f \frac{A_{nt}}{A} \left[ (1 - \sqrt{1 - \phi}) + \frac{\sqrt{1 - \phi}}{1 + \left( \left( 1/\left(\frac{\lambda_s}{\lambda_f}\right) \right) - 1 \right) \sqrt{1 - \phi}} \right] + \left( 1 - \frac{A_{nt}}{A} \right) \times \frac{\lambda_{p,max}^2 \left( \frac{\lambda_{p,max}}{L_0} \right)^{D_T - 1} D_f}{1 + D_T - D_f} \times \left\{ \frac{1}{\gamma_{a1}/\left(\frac{\lambda_s}{\lambda_f}\right) + \frac{(1 - \gamma_{a1})}{\left( \gamma_{c1}^2 \left( \left( \frac{\lambda_s}{\lambda_f} \right) - 1 \right) / \gamma_{a1}^2 \right) + 1}} \right\}$$

where  $A_{nt}/A$ ,  $\gamma_{a1}$ ,  $\gamma_{c1}$ ,  $\lambda_{p,max}$ ,  $L_0$ ,  $D_f$ , and  $D_T$  = fabric parameters describe the particle contact and geometry, and the fractal media.

## References

- Abdel-Hadi, O. N., and Mitchell, J. K. (1981). "Coupled heat and water flows around buried cables." *J. Geotech. Engrg. Div.*, 107(11), 1461–1487.
- Abu-Hamdeh, N. H., Khdaif, A. I., and Reeder, R. C. (2001). "A comparison of two methods used to evaluate thermal conductivity for some soils." *Int. J. Heat Mass Transfer*, 44, 1073–1078.
- Abu-Hamdeh, N. H., and Reeder, R. C. (2000). "Soil thermal conductivity: Effects of density, moisture, salt concentration, and organic matter." *Soil Sci. Soc. Am. J.*, 64, 1285–1290.
- Abuel-Naga, H. M., Bergado, D. T., and Chaiprakaikeow, S. (2006). "Innovative thermal technique for enhancing the performance of prefabricated vertical drain system." *Geotext. Geomembr.*, 24(6), 359–370.
- Anandarajah, A., and Kuganenthira, N. (1995). "Some aspects of fabric anisotropy of soil." *Geotechnique*, 45(1), 69–81.
- Brandon, T. L., and Mitchell, J. K. (1989). "Factors influencing the thermal resistivity of sands." *J. Geotech. Engrg.*, 115(12), 1683–1698.
- Brigaud, F., and Vasseur, G. (1989). "Mineralogy, porosity and fluid control on thermal conductivity of sedimentary rocks." *Geophys. J.*, 98, 525–542.
- Collins, K., and McGown, A. (1974). "The form and function of micro-fabric features in a variety of natural soils." *Pathology*, 24, 223–254.
- Côté, J., and Konrad, J.-M. (2005a). "A generalized thermal conductivity model for soils and construction materials." *Can. Geotech. J.*, 42, 443–458.
- Côté, J., and Konrad, J.-M. (2005b). "Thermal conductivity of base-course materials." *Can. Geotech. J.*, 42(1), 61–78.
- De Vries, D. A. (1963). "Thermal properties of soils." *Physics of plant environment*, W. R. Van Wijk, ed., North-Holland, Amsterdam, The Netherlands, 210–235.
- Farouki, O. T. (1981). *Thermal properties of soils*, CRREL Monograph 81-1, US Army Corps of Engineers, Cold Regions Research and Engineering Laboratory, Hanover, N.H.
- Gera, F., Hueckel, T., and Peano, A. (1996). "Critical issues in modelling of the long-term hydro-thermal performance of natural clay barriers." *Eng. Geol. (Amsterdam)*, 41, 17–33.
- Gori, F., and Corasaniti, S. (2004). "Theoretical prediction of the thermal conductivity and temperature variation inside Mars soil analogues." *Planet. Space Sci.*, 52, 91–99.
- Hadley, G. R., Mcvey, D. F., and Morin, R. (1984). "Thermophysical properties of deep ocean sediments." *Mar. Geotech.*, 5, 257–295.
- Hashin, Z., and Shtrikman, S. (1962). "A Variational approach to the theory of the effective magnetic permeability of multiphase materials." *J. Appl. Phys.*, 33(10), 3125–3131.
- Horai, K. (1971). "Thermal conductivity of rock-forming minerals." *J. Geophys. Res.*, 76, 1278–1308.
- Hsu, C. T., Cheng, P., and Wong, K. W. (1995). "A lumped-parameter model for stagnant thermal conductivity of spatially periodic porous media." *J. Heat Transfer*, 117, 264–.
- Johansen, O. (1975). "Thermal conductivity of soils." Ph.D. thesis, Univ. of Trondheim, Trondheim, Norway.
- Kasubuchi, T. (1984). "Heat conduction model of saturated soil and estimation of thermal conductivity of soil solid phase." *Soil Sci.*, 138, 240–247.
- Kumlutas, D., Tavman, I. H., and Coban, M. T. (2003). "Thermal conductivity of particle filled polyethylene composite materials." *Compos. Sci. Technol.*, 63, 113–117.
- Lambe, T. W. (1958). "The structure of compacted clay." *ASCE Proc.*, 84, 1–34.
- Ma, Y. T., Yu, B. M., Zhang, D. M., and Zou, M. Q. (2003). "A self-similarity model for effective thermal conductivity of porous media." *J. Phys. D*, 36, 2157–2164.
- Martin, R. T., and Ladd, C. C. (1975). "Fabric of consolidated kaolinite." *Clays Clay Miner.*, 23, 17–25.
- Maxwell, J. C. (1954). *A treatise on electricity and magnetism*, 3rd Ed., Dover, New York.
- McConnachie, I. (1974). "Fabric change in consolidated kaolin." *Geotechnique*, 24(2), 207–222.
- McGaw, R. (1969). "Heat conduction in saturated granular materials." *Special Rep. No. 103*, Highway Research Board, 144–131.
- Meade, R. H. (1966). "Factors Influencing the early stages of the compaction of clays and sands-review." *J. Sediment. Petrol.*, 36, 1085–1101.
- Midttømme, K., Roaldset, E., and Aagaard, P. (1998). "Thermal conductivity of selected claystones and mudstones from England." *Clay Miner.*, 33, 131–145.
- Mitchell, J. K. (1993). *Fundamental of soil behavior*, Wiley, New York.
- Mitchell, J. K., and Kao, T. C. (1978). "Measurements of soil thermal resistivity." *J. Geotech. Engrg. Div.*, 104, 1307–1320.
- Morin, R., and Silva, A. J. (1984). "The effect of high pressure and high temperature on some physical properties of ocean sediments." *J. Geophys. Res.*, 89, 511–526.
- Moritz, L. (1995). "Geotechnical properties of clay at elevated temperatures." *Proc. Int. Symp. Compression and Consolidation of Clayey Soils*, IS, Hiroshima, Japan, 267–272.
- Naidu, A. D., and Singh, D. N. (2004). "Field probe for measuring thermal resistivity of soils." *J. Geotech. Geoenviron. Eng.*, 130(2), 213–216.
- Newson, T. A., and Brunning, P. (2004). "Thermal conductivity of deep-water offshore sediments." *Inter. J. Offshore and Polar Eng.*, 14, 310–314.
- Nimick, F. B., and Leith, J. R. (1992). "A model for thermal conductivity of granular Porous media." *J. Heat Transfer*, 114, 505–508.
- Ochsner, T. E., Horton, R., and Ren, T. (2001). "A new perspective on



- soil thermal properties." *Soil Sci. Soc. Am. J.*, 65, 1641–1647.
- Ohtsubo, M., Egashira, K., Koumoto, T., and Bergado, D. T. (2000). "Mineralogy and chemistry, and their correlation with the geotechnical index properties of Bangkok clay: Comparison with Ariake Clay." *Soils Found.*, 40, 11–21.
- Penner, E. (1963). "Anisotropic thermal conduction in clay sediments." *Proc., Int. Clay Conf.*, Stockholm, Sweden, 365–376.
- Reuss, A. (1929). "Berechnung der Fließgrenze von Mischkristallen auf Grund der Plastizitätsbedingung für Einkristalle." *Z. Angew. Math. Mech.*, 9, 49–58.
- Roth, P., Georgiev, A., Busso, A., and Barraza, E. (2004). "First in situ determination of ground and borehole thermal properties in Latin America." *Renewable Energy*, 29(12), 1947–1963.
- Russell, H. W. (1935). "Principles of heat flow in porous insulation." *J. Am. Ceram. Soc.*, 18, 1.
- Sepaskhah, A. R., and Boersma, L. (1979). "Thermal conductivity of soils as a function of temperature and water content." *Soil Sci. Soc. Am. J.*, 43, 439–444.
- Slegel, D. L., and Davis, L. R. (1977). "Transient heat and mass transfer in soils in the vicinity of heated porous pipes." *J. Heat Transfer*, 99, 541–621.
- Tarnawski, V. R., Gori, F., Wagner, B., and Buchan, G. D. (2000). "Modeling approaches to predicting thermal conductivity of soils at high temperatures." *Int. J. Energy Res.* 24, 403–423.
- Valente, A., Morais, R., Tuli, A., Hopmans, J. W., and Kluitenberg, G. J. (2006). "Multifunctional probe for small-scale simultaneous measurements of soil thermal properties, water content, and electrical conductivity." *Sens. Actuators, A*, 132(1), 70–77.
- Yu, B. M., and Cheng, P. (2001). "Fractal models for the effective thermal conductivity of bidispersed porous media." *J. Thermophys. Heat Transfer*, 16, 22.